Divergence/Flutter Suppression System for a Forward Swept-Wing Configuration with Wing-Mounted Stores

M Rimer*, R Chipman,† and R Mercadante‡
Grumman Aerospace Corporation, Bethpage, New York

The conceptual design of an active control system has been developed for a forward swept wing configuration with stores to prevent the destiffening of the primary wing bending mode with increasing airspeed, thereby suppressing the inherent aeroelastic instability (divergence/body freedom flutter). The architecture includes wing mounted and fuselage-mounted accelerometers to detect relative wing motion and an outboard wing flaperon to control this motion By virtually eliminating the instability, the design enables the aircraft to carry significant wing-mounted stores while retaining the clean wing flight envelope On the Control Configured Vehicle (CCV) configuration studied (26% unstable), the system is a simple add on to the existing flight control system and, based on a preliminary assessment, does not compromise longitudinal flying qualities.

Nomenclature

g = gravity constant
K_F = control gain
K_ξ = displacement gain
$K_{\dot\xi}$ = velocity gain
K_I = integrator gain
M = Mach number
M_{CAN} = canard effectiveness
N_Z = vertical acceleration
N_{Z_f} = vertical acceleration at fuselage
N_{Z_w} = vertical acceleration at wing
Q = pitch rate
$\tilde{Q}$ = state quadratic weighting
$\tilde{R}$ = control quadratic weighting
u_c = canard command
u_f = flaperon command
V = airplane velocity
V_D = airplane design velocity
Xl_{WB} = wing first bending displacement
γ = nondimensional damping
ξ = generalized coordinate
ϕ = normal modes
τ = actuator lag
ω = modal frequency

I Background

ON tactical vehicles with aft-swept wings, active control systems which address aeroelastic instability (i e., suppress flutter within a desired flight envelope) have achieved a degree of maturity [1,2] A typical goal of such systems in tactical aircraft retrofits is to make possible an expansion of the store inventory or even of the flight envelope itself Of course, the systems could also be incorporated in original designs to suppress aeroelastic instabilities or to alleviate maneuver/gust loads

Currently, this technology is proposed anew for forward swept wing (FSW) configurations Our initial studies show the fundamental aeroelastic phenomenon of FSW to be the destiffening of the primary wing-bending mode with increasing airspeed It was pointed out[3-5] that, for a wing clamped at its root, this behavior leads to static wing divergence, but for a wing mounted on a vehicle free to fly (unrestrained), the destiffening mode can couple with the short period characteristics of the aircraft causing the dynamic instability known as body freedom flutter (BFF) Therefore, besides the structural integrity issue, there may also be flying quality aspects of BFF depending upon where the instability occurs in relation to the flight envelope

To prevent wing-bending destiffening and the resultant BFF, our previous work[3] formulated the conceptual design of an active divergence/flutter suppression (ADFS) system for an advanced FSW tactical configuration. The system worked by obtaining a measurement of relative wing motion and controlling that motion with an outboard wing flaperon The architecture implied by this work is similar to that used in Ref. 4 and is adopted again in the present paper

In the present paper, this concept is expanded to a CCV tactical configuration with stores The ADFS system is designed as an add-on to a basic flight control system (FCS) that provides longitudinal stability to an otherwise statically unstable aircraft The configuration is such that no ADFS is required for the clean wing, but an ADFS is mandatory if stores are mounted on the wing and the same flight envelope is to be retained Specifically, the present paper describes the proper design criteria, the conceptual design itself, an assessment of the performance of the system, and (to some extent) the impact on flying qualities All these results are representative of FSW technology

II Baseline Configurations

Math Models

Comprehensive dynamic and aerodynamic models of the tactical FSW configurations shown in Fig. 1 were developed Three configurations were considered: the clean wing aircraft, the aircraft with one tip mounted and one underwing Sidewinder, and the aircraft with a tip mounted Sidewinder and two underwing Sparrows A symmetric free-free dynamics model was used to generate both the rigid body modes and the 20 flexible modes lowest in frequency for each

Received Sept 23, 1983; revision received March 21, 1984.

*Senior Engineer Flight Controls
†Engineering Specialist Aeroelasticity Member AIAA
‡Associate Engineer Flight Controls

of the three configurations. Studies were made to reduce each set of modes to a subset appropriate for each of the three configurations. Using the doublet lattice method[9] with store-modeling recommendations evolved in recent years,[7] aerodynamics were computed at $M=0.9$, sea level on all major components of the configurations, i.e., wing, glove, strake, canard, fuselage, store bodies, store fins, store launchers, and pylons. Figure 2 shows the paneling used for one of the configurations.

A state-variable representation of the rigid and flexible equations of motion was generated for each configuration using the Servo Aero Elastics (SAEL) code.[3] These math models were used to design and evaluate both the required FCS and ADFS systems.

Basic FCS

Because the uncontrolled aircraft is highly unstable (static margin of -26%), an FCS was designed to stabilize the baseline clean-wing configuration. Figure 3 shows the FCS block diagram. The basic architecture includes the measurement of vertical acceleration, N_Z, pitch rate, Q, and pitch acceleration, $\dot{Q}$, and uses proportional-plus-integral command to the canard. To assure a design representative of a realistic aircraft, an appropriate two-degree-of-freedom implicit model of the longitudinal flying qualities was used in conjunction with linear quadratic output-state optimal control theory.[8] In particular, the chosen quadratic performance index was:

$$J=\int_{t_0}^{t_f}(\Delta y^T\hat{Q}\Delta y+U^T\hat{R}U)\,dt \qquad (1)$$

where Δy represents the difference between the implicit model responses (vertical acceleration, pitch rate, and pitch acceleration) and the actual aircraft responses, and where the other symbols have their standard meanings. This approach is illustrated schematically in the solid-line portion of Fig. 4. Figure 5 shows the response of the controlled aircraft and the flying qualities model to a 1-g N_Z stick command. As can be seen, the FCS does its job well at the design point ($M=0.9$, sea level); i.e., there are no discernible differences between the model and the aircraft responses. It should be noted that this design was accomplished using only rigid equations of motion with aerodynamic derivatives corrected for flexibility, but was evaluated using the full set of rigid and flexible equations.

Impact of Aeroelastics

For each complete aircraft/stores/FCS configuration, analyses were run to determine the airspeed at which the BFF would occur and, hence, the flutter speed margin. Figure 6 presents velocity root loci of the short-period and primary-wing-bending modes for the three configurations. As can be seen in each case, the wing bending mode destiffens and couples with the short-period mode, causing a dynamic instability. In the clean-wing case, the short-period mode is driven unstable at 33% above the design speed. In the wing/stores cases, the wing bending mode itself goes unstable. The flutter-speed margin is 8% for the two-Sidewinder configuration and 0% for the one-Sidewinder/two Sparrow case—both below the 15% required for military aircraft. Thus, the necessity of an ADFS system for the FSW with stores is confirmed.

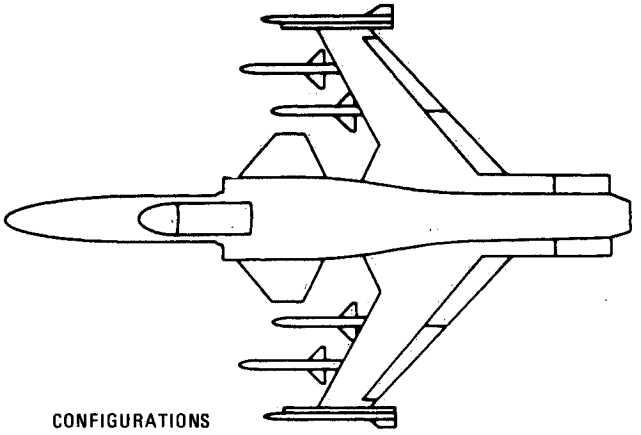

Fig. 1 Configurations for ADFS studies.

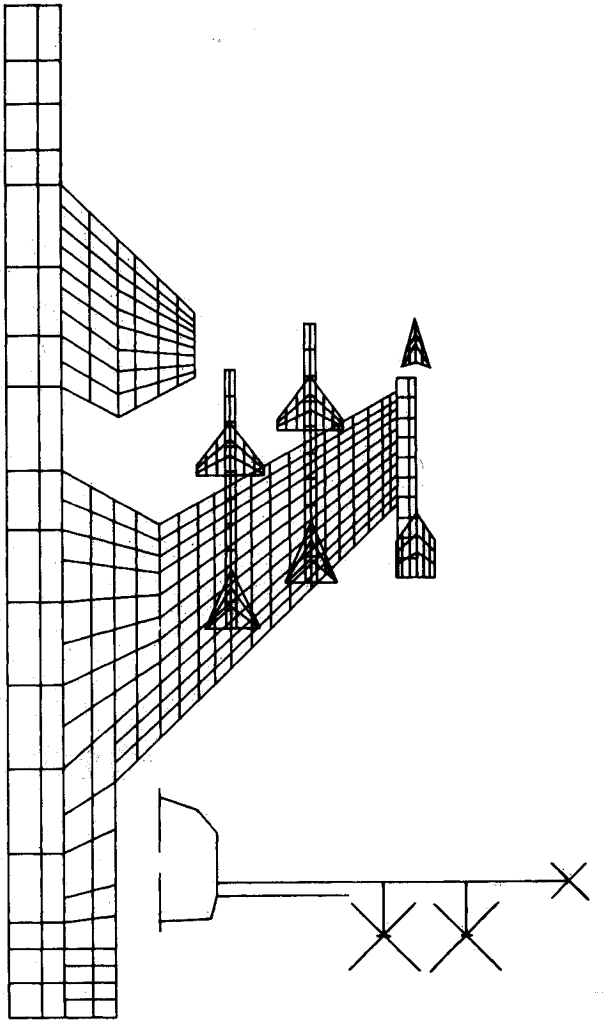

Fig. 2 Aerodynamic paneling of wing-store configuration S2.

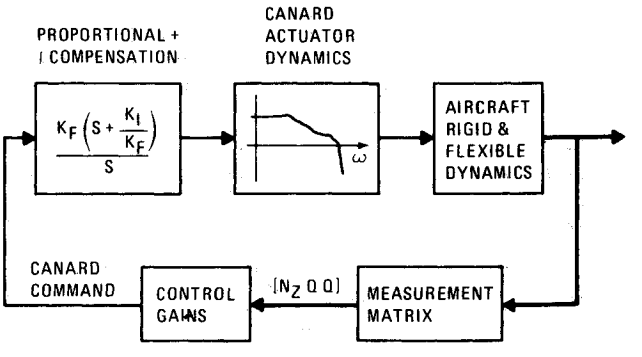

Fig. 3 FCS block diagram.

III Fundamental Mechanisms

To understand the mechanisms involved in BFF more fully and to help delineate design criteria, a reduced version of the state variable model of the system was developed that contained the following salient features necessary to explore the various phenomena: 1) two degree of freedom short-period mode dynamics, 2) third order actuator dynamics for flaperon and canard, 3) primary wing bending-mode dynamics, including aerodynamic destiffening and damping effects, and 4) primary-fuselage mode dynamics with aero destiffening and damping effects

The architecture of the ADFS system is illustrated in the block diagram of Fig 7, which shows the most complex ADFS system considered; i.e , both ξ and $\dot{\xi}$ feedback to the flaperon are used to stabilize the wing mode Reduced order systems studied also include: flaperon control with ξ feedback only, canard control of flexible aircraft, and canard control of rigid aircraft Each of these analyses proved valuable in providing the insight necessary to understand the various phenomena and how they can be best used to improve the final design.

The clean wing BFF velocity locus for the reduced-order model is shown in Fig 8 When this plot is compared with that of Fig 6, it is seen that the clean wing reduced-order locus resembles the wing with stores full-order loci in that the wing-bending mode goes unstable In the clean-wing full order loci, it is the short period mode that goes unstable This is *not* a change of mechanism; in each case the instability is caused by the coupling between the wing bending and short-period modes, and the eigenvector of the unstable mode shows significant participation from both modes In fact, this mode switching phenomenon can be brought about by relatively slight changes in the math modeling of the system. For example, as is discussed below, a variation in wing bending mode damping can trigger such a switch

The basic characteristics of both the full-order and the reduced-order clean wing loci are as follows: At the aircraft design velocity, the wing-bending and short-period eigenvalues are well behaved As the velocity increases, the classic effect of wing destiffening is evident as the bending

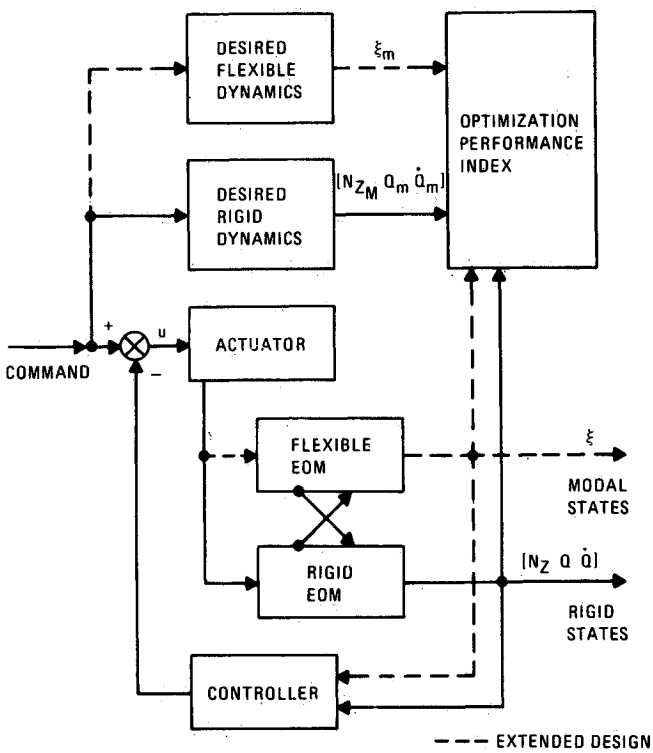

Fig 4 Implicit model block diagram

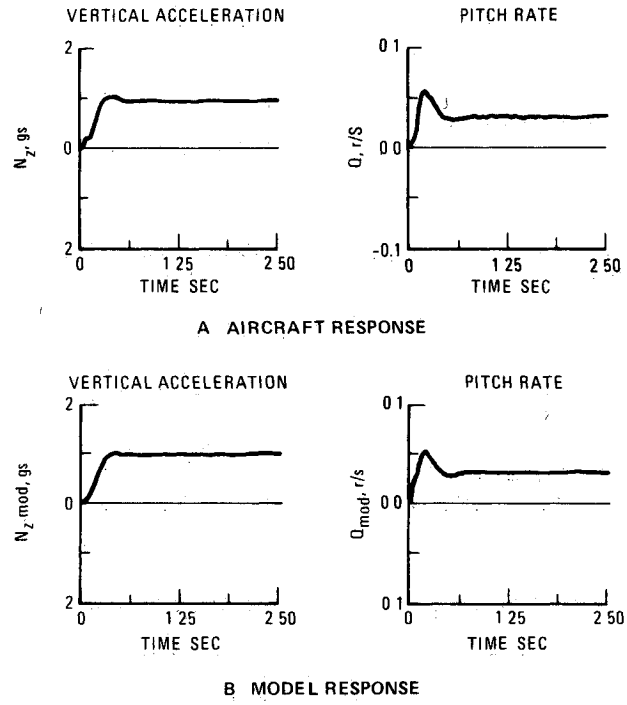

Fig 5 Response to 1-g N_Z step input

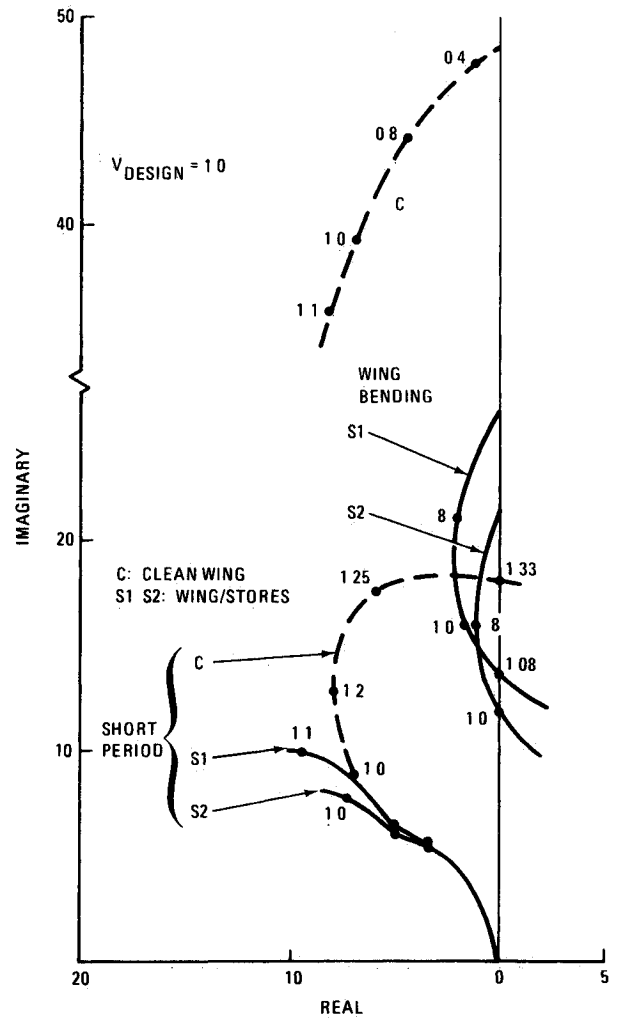

Fig 6 Velocity root loci for three configurations

locus comes down in frequency while simultaneously the short period mode stiffens (or rises) in frequency The initial approach of these modes is slow, but as they near each other and the coupling becomes stronger, small velocity deltas cause large locus changes Ultimately, in the reduced-order locus, the wing mode veers into the right half plane while the short period mode drives left and becomes more stable The trend switches for the full-order modeling.

One might think that if the wing bending mode could be designed to be more highly damped, better performance as indicated by the instability occurring at a higher velocity would result A series of loci exploring this hypothesis (Fig 9) indicates that this is not necessarily the case Variations in damping showed that a separatrix exists in the complex plane, which determines which of the two modes goes unstable Therefore, as the damping is increased (and before much improvement can be achieved due to the wing mode going unstable at a higher velocity), the short period mode takes over and begins to go unstable. These results confirmed the conclusion of Ref 3 that only limited improvement is possible by increasing the wing bending mode damping, i e., that $\dot{\xi}$ feedback alone would be ineffective

It is interesting to note that at this point a different type of separatrix can result if the canard control effectiveness becomes large Figure 10 demonstrates this effect for three different values of M_{CAN} It can be seen that, if the canard is sufficiently powerful, the BFF velocity locus is altered; now the mode that remains stable (be it short period or wing bending) does not become critically damped as velocity is increased Therefore the separatrix, instead of coming down to the negative real axis, would curve up into the complex plane This behavior is caused by the relative position in the S

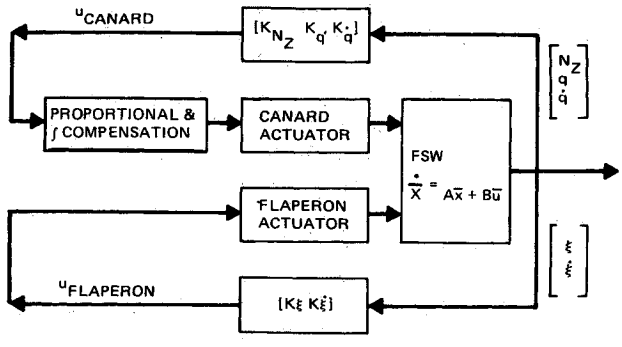

Fig 7 System block diagram

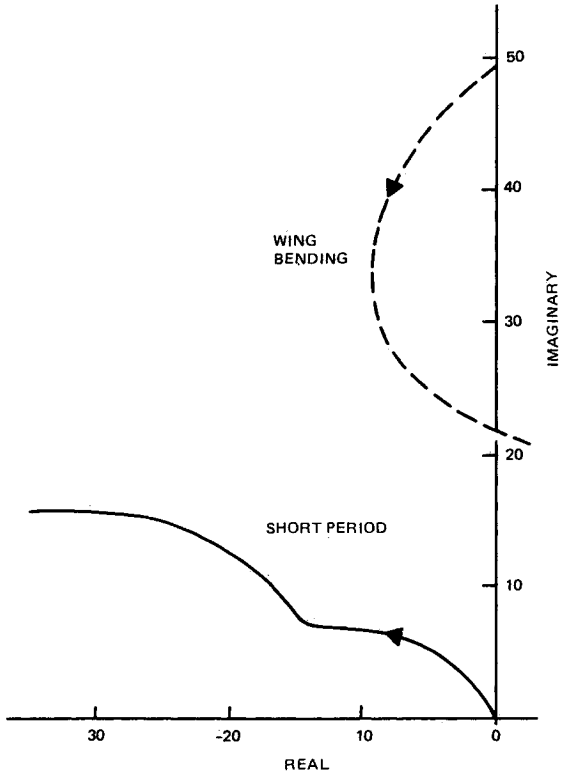

Fig 8 Velocity locus, reduced order model

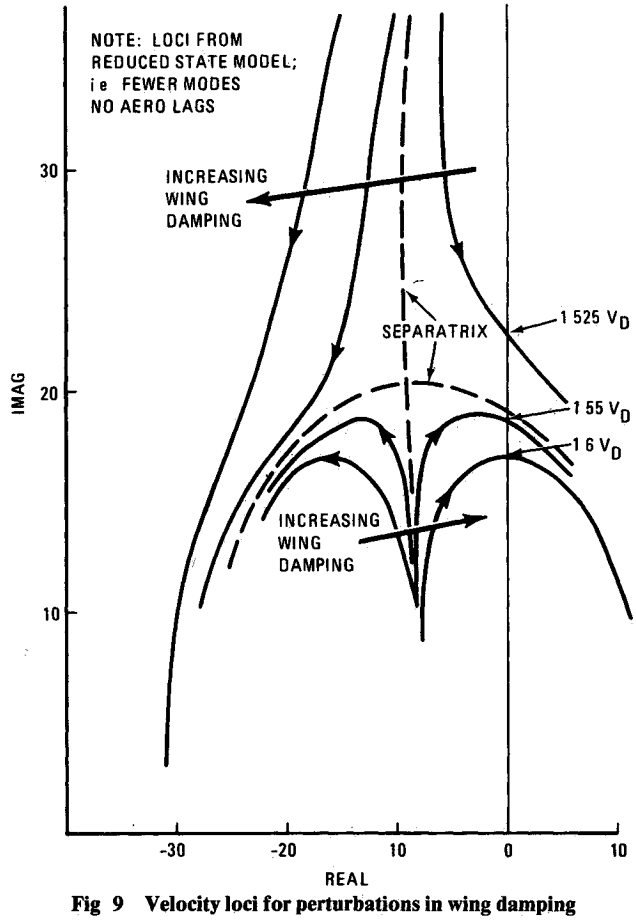

Fig 9 Velocity loci for perturbations in wing damping

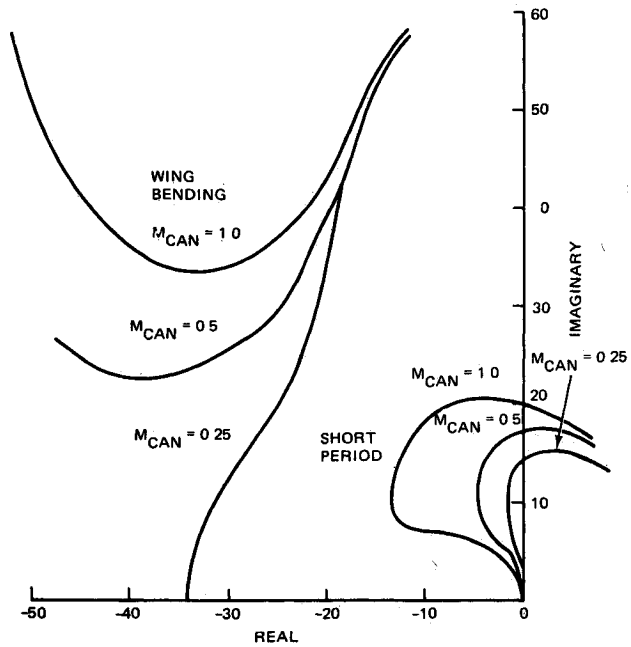

Fig 10 Separatrix, high-control effectiveness

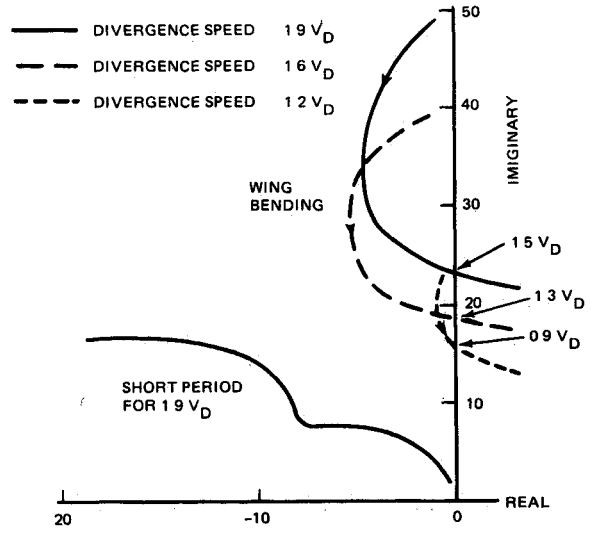

Fig. 11 Velocity loci for variations in wing bending frequency

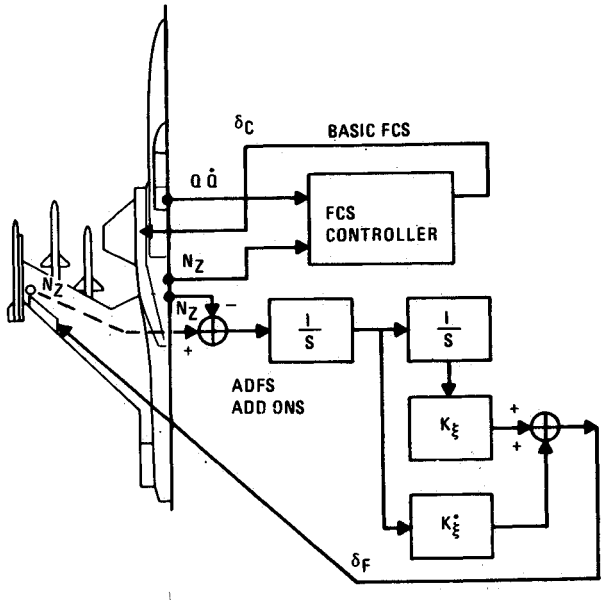

Fig. 12 ADFS architecture

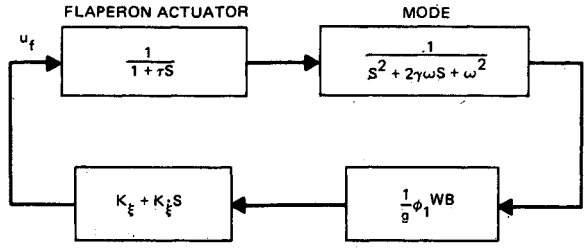

Fig 13 Simplified decoupled wing mode block diagram

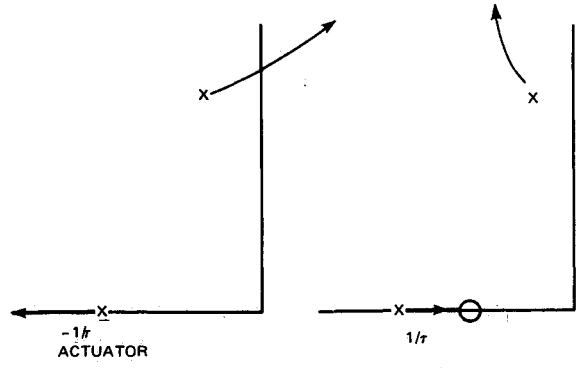

a) ξ feedback. **b) ξ and $\dot\xi$ feedback**

Fig 14 Root locus sketches

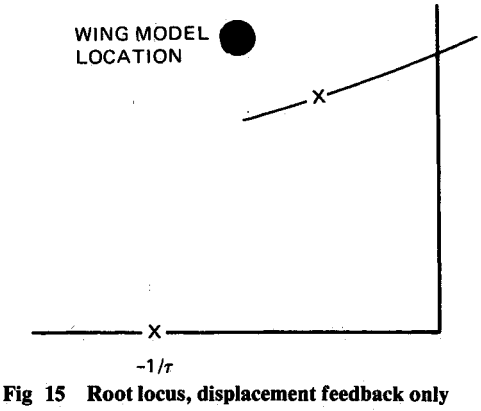

Fig 15 Root locus, displacement feedback only

plane of the actuator pole and the real zero introduced when the feedback loop driving the canard is closed The location of this zero is a function of canard effectiveness When the zero is to the right of the pole, the stable mode will eventually become critically damped; when the zero is to the left (higher canard effectiveness), the mode will remain subcritically damped

Returning our discussion to the prevention of BFF, the next series of runs demonstrated that significant stabilization could be obtained by separating the frequencies of the two coupling modes In these runs, the wing bending dynamics were varied to obtain various divergence speeds These included the nominal case with a divergence speed of 1 9 V_D, a stores case with divergence speed of 1 2 V_D, and an intermediate condition with a divergence of 1 6 V_D Since the wing bending mode is described by a second-order differential equation, its dynamics in state variable form are

$$\dot{\xi} = \begin{bmatrix} 0 & 1 \\ -\omega^2 & -2\gamma\omega \end{bmatrix} \xi \qquad (2)$$

The modal frequency, ω^2, is further described by

ω^2 = (aero stiffness-structural stiffness)/generalized mass

which for the above three cases, is

$$\text{Nominal} \quad 673\left(\frac{V}{V_{\text{DESIGN}}}\right)^2 - 2372$$

$$\text{Mid} \quad 600\left(\frac{V}{V_{\text{DESIGN}}}\right)^2 - 1536$$

$$\text{Stores} \quad 333\left(\frac{V}{V_{\text{DESIGN}}}\right)^2 - 470$$

From these relationships, it is clear the velocity loci for those wing modes with higher divergence speeds will appear at higher frequencies When the BFF velocity loci were

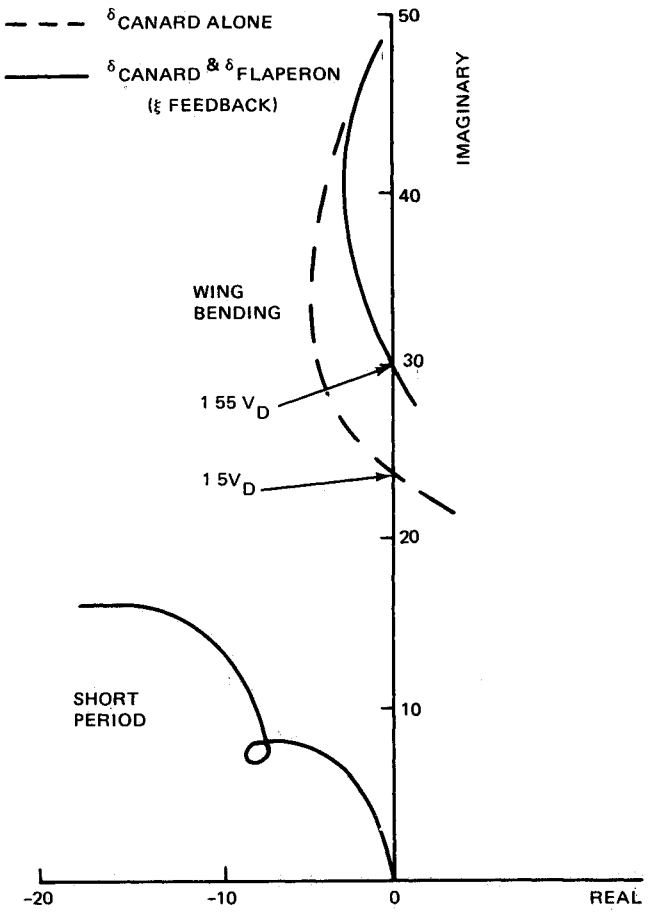

Fig. 16 Suppression system ξ feedback

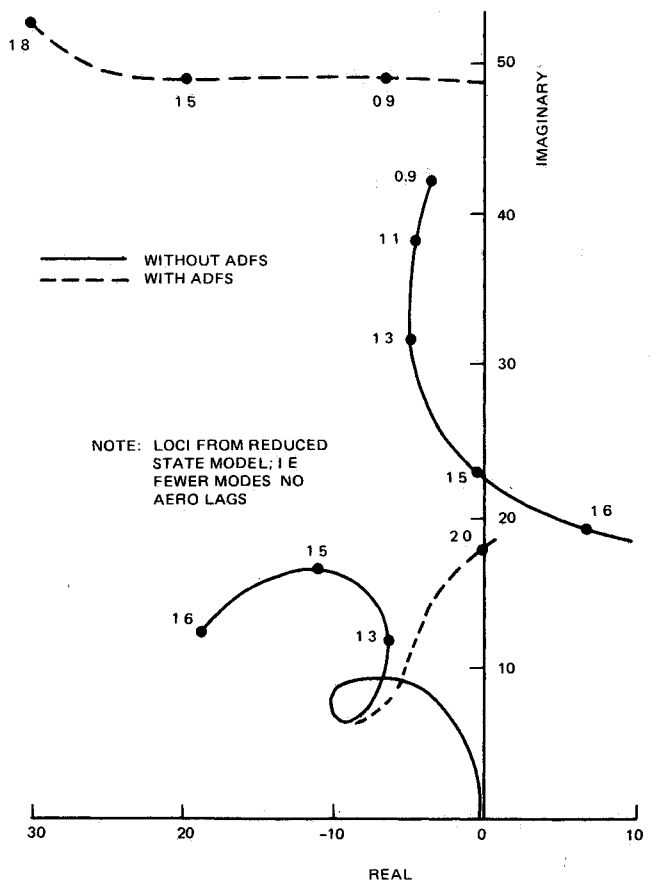

Fig 17 Velocity loci, clean wing

generated for these cases (see Fig 11), the benefits of separating the frequencies became evident as the BFF in stability velocities went from 0 9 V_D in the stores case to 1 5 V_D for the nominal case

It must be emphasized that similar gains are achievable by holding the wing frequency constant and lowering that of the short-period mode, but this is usually not a desirable design procedure as this tampers with the basic aircraft handling qualities

The criteria for a proper design are now in place: provide the proper augmentation to stiffen the wing bending mode (raise its frequency), desensitize it to velocity changes, and do not change the basic short period mode characteristics

IV ADFS Design

Architecture

The control system architecture formulated to allow the above goals to be met is illustrated in Fig 12 As can be seen, the ADFS is essentially a wraparound to the basic FCS An acceleration sensor is located out on the wing, near both the controller and a torsional node line This colocation of the sensor/actuator is good design practice to provide for stable interactions for all modes, while the location near the tor sional node line lessens the chances of unwanted modal couplings Each accelerometer registers the following,

$$N_{Z_w} = \frac{1}{g}(-\dot{W} + VQ - \Delta x_1 \dot{Q} - \phi_1^{WB\xi WB})$$

$$N_{Z_f} = \frac{1}{g}(-\dot{W} + VQ - \Delta x_2 \dot{Q} - \phi_2^{WB\xi WB}) \qquad (3)$$

Since both sensors are located at the same fuselage station, $\Delta x_1 = \Delta x_2$; in addition, $\phi_2^{WB} \simeq 0$ By forming the difference of the two sensors, the desired signal is generated:

$$N_{Z_w} - N_{Z_f} \simeq -\frac{1}{g}\phi_1{}^{WB\xi WB} \qquad (4)$$

We now have a control structure capable of both observing and controlling the structural mode of interest A simplified block diagram of the wing mode, decoupled from the short-period mode, with the above system is shown in Fig 13

Root locus sketches (Fig 14) derived from inspection of Fig 13 illuminate how ξ and $\dot{\xi}$ feedback affect the desired stiffening of the wing mode Figure 14a illustrates that ξ feedback alone provides only limited stiffening at the expense of lower damping On the other hand, feeding back both ξ and $\dot{\xi}$ allows the designer to shape the locus (by positioning the compensation zero) and to pick the operating point (by setting the loop gain) Even though we are dealing with a multivariable coupled system, these trends should be obvious during the design procedure.

ADFS Synthesis

The ADFS design was performed employing linear quadratic optimization techniques and, in particular, using output state feedback A unique feature of the optimization design was the use of an implicit model of the wingbending mode in the system state cost functional A second order model was constructed whose form was as in Eq (2), but with the desired frequency and damping characteristics. The resulting control gains should theoretically locate the actual mode root where the implicit model root lies This is true for the full state feedback solution, but not necessarily for the partial state case Using ξ feedback alone, the optimization process could do very little in stiffening the bending mode. Of course, the main reason for this is explained by referring to Fig 14a The goal was that the mode be at a higher frequency and damping (see Fig 15), but the potential space where it could be placed by the ξ gain was along the indicated line.

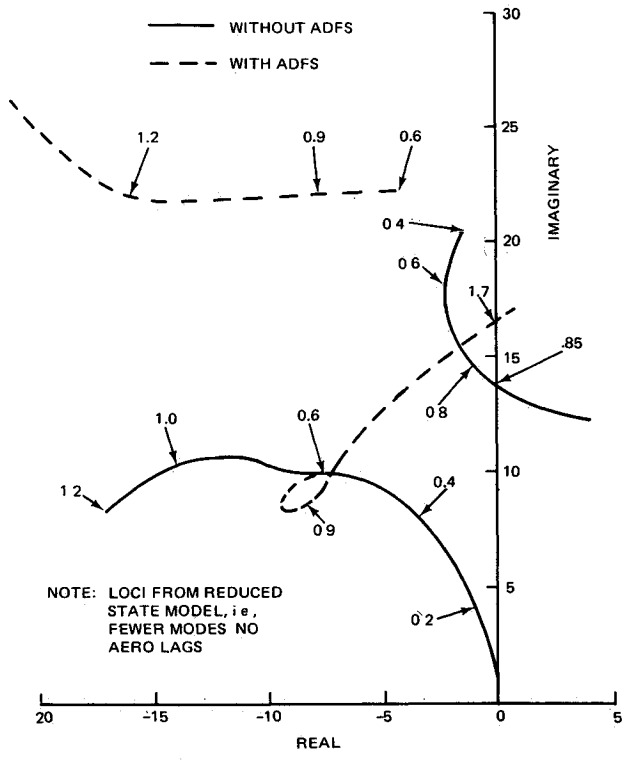

Fig 18 Velocity loci, wing with stores

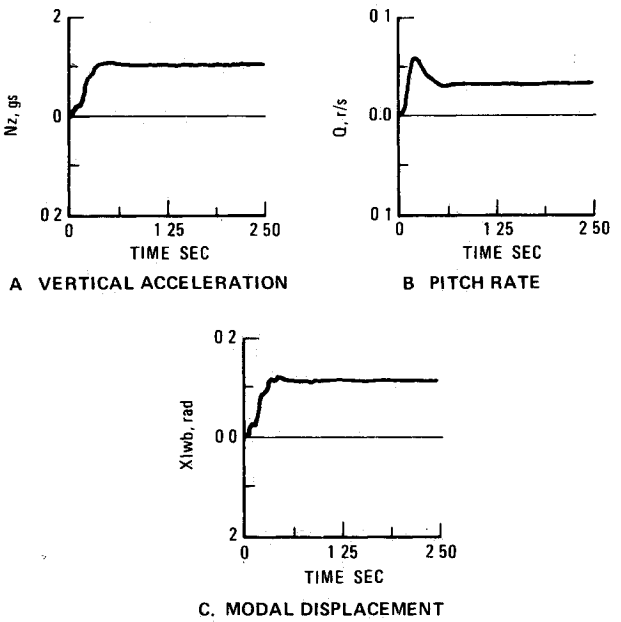

Fig 19 Response to 1-g N_Z step with ADFS

A velocity locus for the best set of gains is shown in Fig 16; the original locus is also plotted in this figure for comparison purposes A small increase in velocity margin (3%) is achieved due to ξ feedback By comparing equivalent velocity points between the two loci, the general shape of Fig 15 becomes evident The short period mode locus is left virtually undisturbed with or without the added flaperon control In general, the use of ξ feedback alone does not offer sufficient improvement in the system performance

The picture is totally different when $\dot{\xi}$ feedback is also implemented Once again, output state feedback linear optimization design was performed to determine the system gains The resultant velocity locus is plotted in Fig 17, along

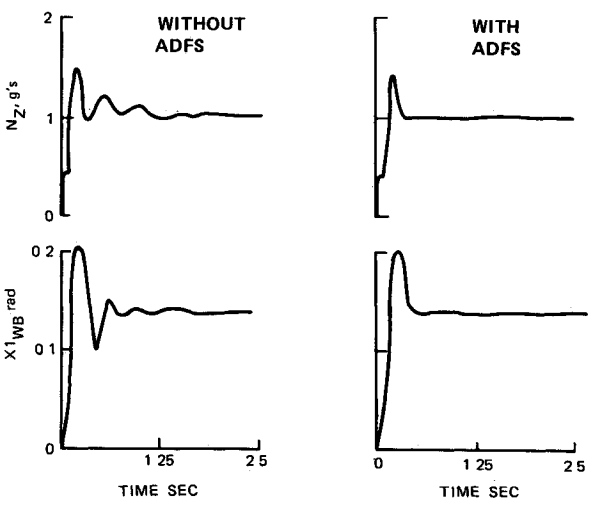

Fig 20 Aircraft response near flutter boundary

with the nominal case for comparison The optimization procedure was able to place the bending mode near the implicit model's frequency and damping, thereby decoupling it from the rigid body short period mode In addition, ξ and $\dot{\xi}$ feedback cause the wing bending velocity locus to move to higher frequencies and damping for higher velocities, further minimizing its detrimental effects The mechanism necessary to produce BFF has clearly been circumvented The eventual instability of the rigid body at 2 0 V_D (33% improvement) is not due to BFF, but is simply the basic short period instability.

A final study was performed to demonstrate that the same design would be successful for a wing loaded with stores The same control architecture and the same feedback gains were used, i e , a reoptimization procedure was not performed The results (Fig 18) were just as successful as for the clean wing configuration In fact, on a percent improvement basis, this compensation appeared more striking: 100% improvement from 0.85 V_D to 1 7 V_D Once again, it is the basic air frame/FCS short period instability and not BFF that limits the improvement

Impact on Flying Qualities

The impact of ADFS on longitudinal flying qualities was assessed in a preliminary fashion by two measures First, as mentioned above, the location of the short-period root at the design velocity was examined with and without ADFS, and was found to be unaffected by the presence of ADFS Second, time histories of the clean wing aircraft response to a 1 g N_Z step command were generated with and without ADFS at the design velocity and at a higher velocity ($V/V_D = 1$ 3) near BFF On comparing Fig 5 (design velocity, no ADFS) with Fig. 19 (design velocity, ADFS on), no degradation in the response is seen In fact, a low amplitude oscillatory component barely apparent without ADFS is entirely absent to the eye when ADFS is employed This is, of course, the suppressed wing-bending mode contribution At the higher velocity (Fig 20), the comparison between response with and without ADFS is much more striking Without ADFS, the effect of the poorly damped short period mode is evident in both the vertical acceleration and wing first bending mode traces When the same input is supplied to an aircraft with an active ADFS system, the improvement is quite dramatic in that all traces of BFF have been eliminated

V Conclusions

An ADFS system was designed for a CCV tactical FSW configuration It is concluded that the system can virtually

preclude the occurrence of the generic BFF instability, thereby making possible the carriage of underwing stores while retaining the clean wing flight envelope The aircraft's stability limit then reverts to the speed at which the basic airframe/FCS short-period instability occurs A cursory assessment of longitudinal flying qualities showed that the addition of ADFS was beneficial in that an undesired modal contribution to the aircraft response was dramatically reduced

References

[1]Hoenlinger H and Lotze A Active Suppression of Aircraft Flutter, Paper presented at the 11th ICAS Congress Lisbon, 1978

[2]Noll, T et al Active Flutter Suppression Design and Test A Joint U S F R G Program Paper ICAS 80 5 5 *ICAS Proceedings* edited by J Singer and R Staufenbiel 1980 pp 232 241

[3]Chipman, R Zislin A , and Waters C Active Control of Aeroelastic Divergence AIAA Paper 82 0684 May 1982

[4]Miller G Wykes J and Brosnan, M , ' Rigid Body Structural Mode Coupling on a Forward Swept Wing Aircraft AIAA Paper 82 0683 May 1982

[5]Weisshaar T , Zeiler T , Hertz T , and Shirk, M Flutter of Forward Swept Wings Analysis and Test AIAA Paper 82 0646 May 1982

[6]Giesing J Kalman T and Rodden W , 'Subsonic Unsteady Aerodynamics for General Configurations ' AFFDL TR 71 5, Part I Feb 1971

[7]Tijdeman, H et al 'Transonic Wind Tunnel Tests on an Oscillating Wing with External Stores AFFDL TR 78 194 Parts I IV 1979

[8]Gran, R Berman, H and Rossi M ' Optimal Digital Flight Control for Advanced Fighter Aircraft ' *Journal of Aircraft* Vol 14 Jan 1977 pp 32 37